Available online at www.sciencedirect.com
ScienceDirect
International Journal of Heat and Mass Transfer 51 (2008) 724–735
International Journal of HEAT and MASS TRANSFER
www.elsevier.com/locate/ijhmt

The influence of secondary refrigerant air chiller U-bends on fluid temperature profile and downstream heat transfer for laminar flow conditions

Richard Clarke, Donal P. Finn *

School of Electronic, Electrical and Mechanical Engineering, University College Dublin, Belfield Dublin 4, Ireland

Received 26 June 2006
Available online 14 August 2007

Abstract

This paper describes numerical investigations, using computational fluid dynamics, conducted to examine the heat transfer mechanisms by which air-chiller U-bends cause enhanced downstream internal convection, where single phase secondary refrigerants under laminar conditions are employed as the heat exchanger fluid. The numerical model, created using FLUENT, consists of a single heat exchanger tube pass incorporating an inlet pipe, a U-bend and an outlet pipe. The model was validated using experimental data from the literature. Numerical investigations indicate that within the U-bend, secondary flows partially invert temperature profiles resulting in a significant localised decrease in average fluid temperature at the pipe surface. As a result, downstream heat transfer enhancement is observed, the magnitude of which can exceed that typical of a pipe combined entry condition in some circumstances by greater than 20% for up to 20 pipe diameters downstream. Heat transfer enhancement was found to increase with increasing U-bend radius, but to decrease with increasing heat exchanger pipe radius and internal Reynolds number. A simple technique based on quantification of the degree of temperature inversion at the U-bend is proposed which provides a mechanism by which heat transfer enhancement can be estimated.

Keywords: CFD; Heat transfer enhancement; Laminar; Secondary refrigeration; Temperature profile; U-bend

1. Introduction

Indirect refrigeration systems (Fig. 1), often used in supermarket applications [1,2], present an alternative refrigeration design concept to direct expansion (DX) systems that can reduce, or even eliminate, the use of environmentally damaging CFC (chlorofluorocarbon), HFC (hydro-fluorocarbons) and HCFC (hydro-chlorofluorocarbon) refrigerant compounds. A major advantage of this system is that a smaller quantity of refrigerant is required in the primary loop than would be required if a direct expansion (DX) system alone were used. Horton and Groll [1] compared a DX system to an indirect system with an equivalent cooling capacity. The charge of primary refrigerant required for the indirect system was only 10% of the refrigerant charge required for the DX system.

Indirect refrigeration systems however, require an additional heat exchanger and a secondary refrigerant pump, typically resulting in increased energy requirements over equivalent DX systems [3]. In addition, a common feature of most antifreeze secondary refrigerants is that they operate in single-phase mode. Consequently, the high convection heat transfer coefficients associated with the evaporation of a fluid is unavailable. Recent studies into secondary refrigeration systems however, have determined that they can be surprisingly effective under the laminar flow regime, even outperforming direct expansion alternatives [4]. Laminar flow, typically associated with poor heat transfer, has been found by Haglund Stignor, [5] to provide the most energy efficient air-chiller performance in many

* Corresponding author. Tel.: +353 1 7161947; fax: +353 1 283 0534.
E-mail address: donal.finn@ucd.ie (D.P. Finn).

0017-9310/$ - see front matter © 2007 Elsevier Ltd. All rights reserved.
doi:10.1016/j.ijheatmasstransfer.2007.04.047

Nomenclature

C_p	specific heat capacity (J kg^{-1} K^{-1})
D	pipe diameter (mm)
e	percentage error (%)
Gr	Grashoflf number $= g\beta(T_s - T_m)\delta^3 v^{-2}$
h	convection heat transfer coefficient (W m^{-2} K^{-1})
k	thermal conductivity (W m^{-1} K^{-1})
K	Dean number
L_i	inlet pipe length (m)
L_o	outlet pipe length (m)
Nu	Nusselt number $= hDk^{-1}$
Pr	Prandtl number $= \mu C_p k^{-1}$
Q	surface heat flux (W m^{-2})
r	pipe radius (mm)
R	bend radius (mm)
Re	Reynolds number $= \rho VD/\mu$
T	temperature (K)
V	fluid velocity (m s^{-1})
x	axial distance along pipe (m)
x^*	dimensionless distance $= x/D\,Re\,Pr$

Greek symbols

β	coefficient of thermal expansion (K^{-1})
θ	sector angle (°)
μ	viscosity (kg m^{-1} s^{-1})
ν	kinematic viscosity (m^2 s^{-1})
ρ	density (kg m^{-3})

Subscripts

exp	from experimental data
in	at inlet
i	at circumferential location i
m	mean
max	maximum
min	minimum
out	at outlet
sim	from simulation
tot	total
w	at pipe wall
x	at axial location, x

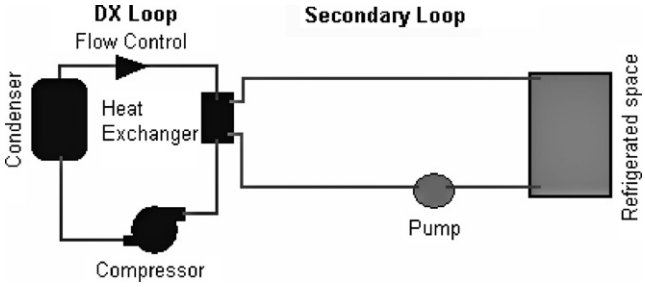

Fig. 1. Indirect refrigeration system.

situations, due to surprisingly good heat transfer performance and the reduced pumping power required for laminar flow. Hong and Hrnjak [6] proposed that secondary flows developed within air chiller pipe bends cause significant mixing of the flow. This effect, it is suggested, eliminates the hydrodynamic and thermal development that occurs prior to the bend, resulting in a new development length immediately downstream of the U-bend. Within the development region, which extends to a significant length for high Pr number secondary refrigerant fluids, high convective heat transfer can exist for laminar flow conditions. Specific investigation of the precise transport mechanisms that cause this heat transfer enhancement however, remain to be conducted and this forms the basis for the current research.

Other experimental investigations conducted to date [7–10] have found that heat transfer may be enhanced immediately downstream of a U-bend. Unlike the current study, these investigations concentrated upon the magnitude of the enhancement effect and not upon the transport mechanisms that cause it. In general, the heat transfer enhancement is attributed to the mixing effect of centrifugally induced secondary flows known as Dean Vortices that develop within the bend. These secondary flows, first described by Dean [11,12], are a result of centrifugal forces and a transverse pressure gradient that develop within the pipe as a fluid traverses a bend. Secondary flows have been characterised by a dimensionless number $K = Re\sqrt{(r/R)}$, the Dean number [13]. The heat transfer enhancement effect of the secondary flow downstream of a bend is most pronounced for laminar flow, [7,8] under which conditions heat transfer can also be influenced by natural convection [8,9]. Moshfeghian [8] noted that the surface temperatures following the bend vary circumferentially and suggested that it is the redistribution of temperature that occurs within the bend that leads to the downstream heat transfer enhancement.

Abdelmessih and Bell [10] proposed a correlation (Eq. (1)) for the local Nusselt number following U-bends. This correlation attempts to incorporate the effects of forced convection, natural convection and secondary flow effects and is based on experimental data that lies within the ranges: $120 \leqslant Re \leqslant 2500$; $3.9 \leqslant Pr \leqslant 110$; $2500 \leqslant Gr \leqslant 1{,}130{,}1000$; $27 \leqslant x/D \leqslant 171$.

$$Nu = \left[4.36 + 0.327(GrPr)^{1/4} + 1.955 \times 10^{-6} Re^{1.6} K^{0.8} e^{-0.0725(x/D)}\right] \times \left(\frac{\mu_m}{\mu_w}\right)^{0.14} \quad (1)$$

This correlation is applicable to the region downstream of a U-bend and exhibits the impact of the bend through incorporation of the Dean number, K. The influences of

variable properties are taken into account using the ratio of viscosity at both bulk and wall temperatures as suggested by Sieder and Tate [14]. The equation has an absolute average percentage deviation from the experimental data of ±9.9%.

Zitny et al. [15] examined heat transfer enhancement downstream of a U-bend using computational fluid dynamics software and determined that a U-bend has a similar effect to an idealised model of a flow inverter with a wall layer, thus suggesting that a heat transfer enhancement downstream of a U-bend is a result of a flow inversion process. Similar to the experimental work described earlier, these numerical investigations concentrated upon the magnitude of the enhancement and not upon the manner in which the flow is redistributed within the bend and the underlying heat transfer enhancement transport mechanisms.

While the work conducted to date has suggested mechanisms for the heat transfer enhancement that occurs downstream of a U-bend, these mechanisms have not been confirmed or investigated in detail. Hong and Hrnjak [6] suggested that secondary flows potentially cause flow mixing, thereby creating a new development length downstream of the bend somewhat similar to a combined entry situation. Moshfeghian [8] however, notes that the surface temperatures vary circumferentially both within and downstream of the bend. This suggests that while the fluid is redistributed within the bend, it is not mixed sufficiently to result in a homogenous temperature at the bend exit, as is the case for a combined entry. The current work therefore has been motivated by the requirement for a greater understanding of the transport mechanisms that cause this heat transfer enhancement effect. By examining the developing temperature profile both within and downstream of the U-bend, a more complete understanding of the enhancement mechanisms may be developed.

This work aims to advance the fundamental understanding of the transport mechanisms by which U-bends distort temperature profiles under laminar flow conditions within a heat exchanger and consequently enhance downstream heat transfer.

2. Approach

The investigation was conducted using the FLUENT CFD software package. Model geometries were assembled and meshed using the GAMBIT software package and were exported to FLUENT for completion of pre-processing and for solving. The model mesh and solving procedure was validated as outlined in Section 3. The method employed facilitated the observation of velocity vectors and temperature contours upstream of, within and downstream of the U-bend, without the necessity for the use of any potentially intrusive measurement equipment. In this way, it was possible to examine the manner in which U-bends distort the temperature profile of secondary refrigerants in the pipes of secondary refrigerant air-chillers. Furthermore, the approach allowed quantitative assessments of the underlying transport processes to be undertaken.

2.1. The model geometry

The model geometry consisted of a U-bend preceded by a straight circular inlet pipe and followed by an identical straight circular outlet pipe. A number of key dimensions, illustrated in Fig. 2, were varied between different models during both the validation stages and the later investigations conducted to examine the transport mechanisms that drive the heat transfer enhancement effect. For the validation models, dimensions were obtained directly from the source literature [6,9]. For the subsequent investigations, dimensions typical of heat exchangers designed specifically to act as secondary refrigerant air chillers were selected. Haglund Stignor [5] conducted a parameter study of various air-chiller designs and found a heat exchanger, with a pipe diameter of 10 mm and a straight pipe length between U-bends of 500 mm, to be the most energy efficient of a number of designs examined. As a result these dimensions ($L_i = L_o = 500$ mm, $2r = 10$ mm) were selected for the models investigated in this study. A number of bend radii ($R = 12.5$, 15, 20 mm) were employed in order to examine the effect of the ratio of bend to pipe radius upon the downstream heat transfer enhancement mechanism.

2.2. Simulation details

A mesh boundary layer of fine volume elements was created at the pipe circumferential surface. This layer provided greater accuracy of results at the pipe surface at which precise surface temperature data was required in order to determine surface heat transfer and Nusselt (Nu) number values. The boundary layer consisted of four layers of elements and extended to a total depth of 0.54 mm. These boundary layer dimensions provided sufficiently accurate surface data without increasing computing requirements and solving times excessively. The mesh boundary layer is given in Fig. 3 in which the inlet face mesh is illustrated.

The inlet face was meshed using a PAVE scheme that created an unstructured face mesh of quadrilateral elements [16]. This scheme could be readily applied to the inlet geometry region and resulted in a face mesh that was suitable for use with the Cooper volume-meshing scheme. The

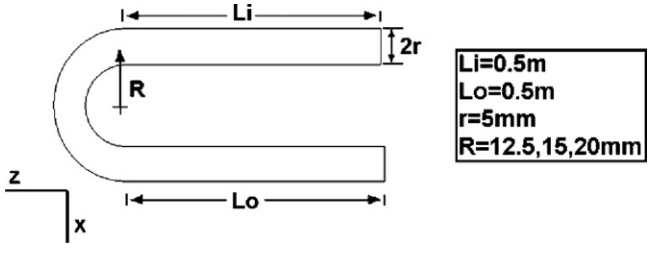

Fig. 2. Key model dimensions.

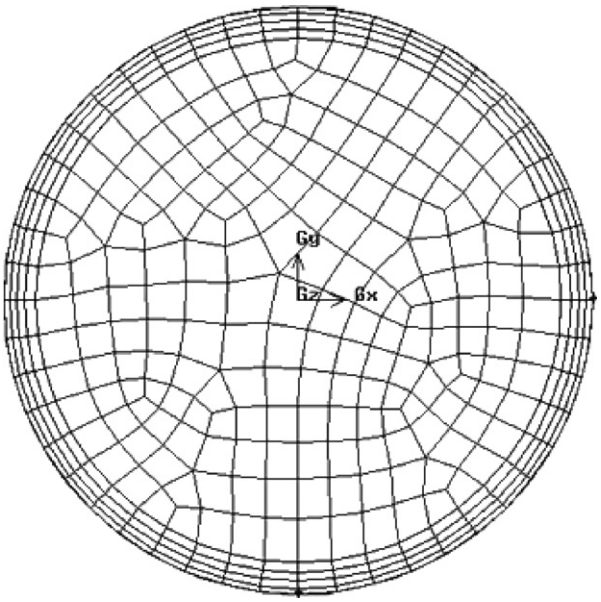

Fig. 3. Inlet face mesh.

hexahedral core formed using the Cooper scheme [17] was structured in the direction of flow in an attempt to minimise numerical diffusion effects. The fully meshed models contained approximately 660,000 volume elements.

A mass flow rate boundary condition was specified at the inlet to the pipe in order to control the fluid flow and *Re* number. This boundary condition applied a constant velocity and temperature at the pipe inlet that was consistent with the conditions associated with a combined entry situation. The fluid was specified as a potassium formate solution for which thermally dependent properties (density, viscosity and thermal conductivity) were specified using user-defined functions written in the C programming language. Potassium formate material properties were identical to those used by Hong and Hrnjak [6] defined by Eqs. (2)–(4). A constant value for specific heat capacity was specified because specific heat capacity varied by less than 1% between fluid temperatures at the inlet and outlet. A value, suitable for the range of temperatures experienced over the length of the pipe, was selected as $C_p = 2550$ J/kg K.

$$\rho = -0.530754 * (T - 273.16) + 1328.7 \quad (2)$$

$$\mu = 0.0000899 * (\exp(479.09/(T - 273.16 + 126.55))) \quad (3)$$

$$k = 0.001674 * (T - 273.16) + 0.4750 \quad (4)$$

Based on the experimental work of Haglund Stignor [5] and Hong and Hrnjak [6], it was found that typical heat fluxes for secondary refrigerant air-chillers reside within the range from 10 to 20 kW m^{-2}. A constant heat flux of 20 kW m^{-2} was specified on the walls and provided a temperature rise over a 1 m pipe section of 6–13 K for $Re = 1500$–500, respectively. The specification of a constant heat flux boundary condition was consistent with the approach employed in the experimental work conducted by both Moshfeghian [8] and Mehta [9]. Furthermore, specification of a constant surface heat flux facilitated the calculation of the fluid mean temperature and the local convective heat transfer coefficient at a circumferential location (denoted by i) on the pipe surface at an axial distance (denoted by x) along the pipe, using Eqs. (5) and (6), respectively. The outlet boundary condition was set as an outflow condition. The outflow boundary condition applies a zero diffusion flux for all flow variables and an overall mass balance correction. Gravity was specified in the *Y*-direction such that the pipe U-bend was orientated in the horizontal plane. A steady, laminar flow model was utilised for which momentum and mass are conserved.

$$T_{m,x} = T_{m,in} + \frac{(T_{m,out} - T_{m,in})\mathbf{x}}{\mathbf{x}_{tot}} \quad (5)$$

$$h_{i,x} = \frac{Q}{T_{w,i,x} - T_{m,x}} \quad (6)$$

3. Model validation

The model and solving procedure were validated by comparison with experimental data from two sources in the literature [6,9]. Data from Hong and Hrnjak [6] was particularly suitable for validation as, similar to the current investigation, the study dealt with the heat transfer from secondary refrigerants downstream of an air-chiller U-bend. Additionally, the secondary fluids investigated by Hong and Hrnjak included the fluid investigated in the current investigation, a potassium formate solution. The secondary refrigerants inside the pipe was heated by warm water flowing in an annulus surrounding the pipe. This situation was assumed for the purposes of the current work to approach that of a constant surface heat flux boundary condition. Measurements were however only available at three axial locations downstream of the U-bend and the small quantity of available data resulted in the use of a second set of validation data from the investigations of Mehta [9], from which a greater quantity of data, in the form of surface temperature values was available. Mehta applied a constant surface heat flux to the tube walls by means of electrical resistance heating. The tube radius (15.75 mm) and bend radius (60 mm) of Mehta's test pipe were larger than those typical of an air-chillers and the fluid used was an ethylene glycol solution. While these slight variations between the experimental tests conducted by Mehta and the numerical investigations conducted for this work subsequent to the validation procedure were not desirable, they provided confirmation of the capability of the numerical method to deal with variations in model parameters and operating conditions.

3.1. Validation against data from Hong and Hrnjak

Surface heat transfer coefficient and *Nu* number data for laminar flow potassium formate, following a U-bend in a

heated pipe were available from Hong and Hrnjak [6]. A numerical model to represent the investigations of Hong and Hrnjak was created in FLUENT as per the procedure outlined in Section 2. Local heat transfer coefficients were determined for eight circumferential locations at 750 axial positions on the inlet and outlet pipes using Eq. (6). Circumferentially averaged local heat transfer and *Nu* number values were determined as per Eqs. (7) and (8).

$$h_{m,x} = \left(\frac{\sum_{i=1}^{8} h_i}{8} \right)_x \tag{7}$$

$$Nu_{m,x} = \frac{h_{m,x} D}{k} \tag{8}$$

Local *Nu* number values, as predicted by Fluent for the outlet pipe, compared to similar data from Hong and Hrnjak are illustrated in Fig. 4. A curve fit for the experimental data used by Hong and Hrnjak is also included in the figure. The choice of curve fit was influenced by the assumption of a large Nusselt number at the entrance region of the pipe. The percentage difference between the experimental data and the simulation data was calculated using Eq. (9) and the average difference, over the range of values of x^* for which experimental data was available ($x^* = 0.00075$–0.0032), was found to be 2.75%. In general, simulation values were found to be less than experimental data suggesting that any small errors present were on the conservative side and did not lead to over-prediction of the enhancement effect.

$$e = 100 \frac{|Nu_{sim} - Nu_{exp}|}{Nu_{exp}} \tag{9}$$

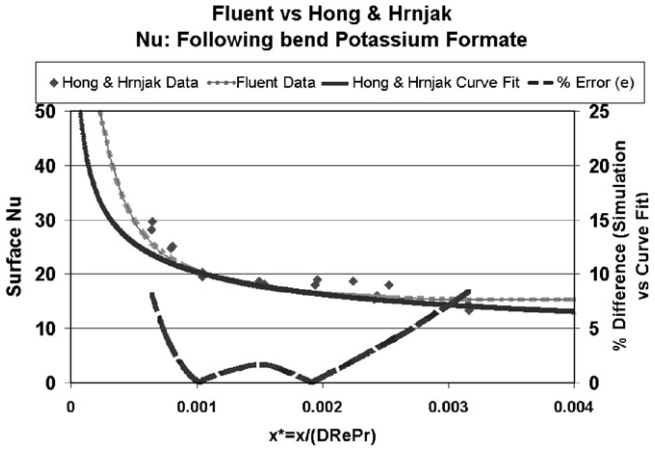

Fig. 4. Validation against Hong and Hrnjak.

3.2. Validation against data from Mehta

Surface temperature data along the length of the outlet pipe at eight evenly spaced circumferential locations was available from the work of Mehta and validation was also performed using this data. A separate numerical model was constructed to represent the investigations of Mehta using the procedure outlined in Section 2. Fig. 5 shows surface temperature data for one such circumferential location, along the top surface of the outlet pipe (line 1) for both a numerical simulation and the experimental work of Mehta. Both data sets compared well with each other for all eight circumferential locations, with a maximum difference for all circumferential and axial locations of 1 K and an average difference of <0.5 K.

It was concluded from this validation process that the simulation procedure and model mesh was capable of

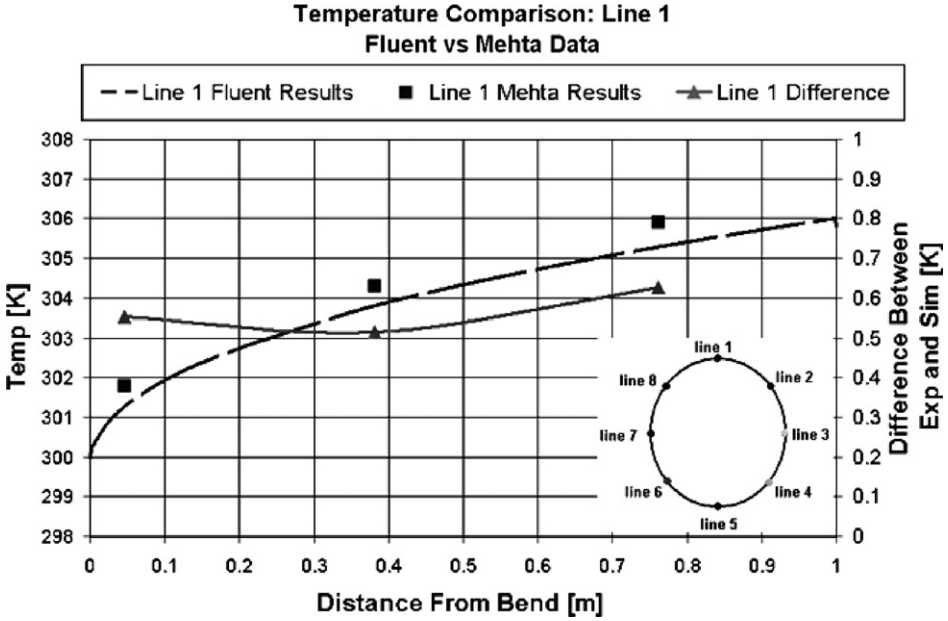

Fig. 5. Validation against Mehta data.

modelling the heat transfer enhancement of laminar flow fluids downstream of a U-bend sufficiently accurately to justify their use for further investigations into the transport mechanisms that cause this enhancement.

4. Results

For high *Pr* number secondary refrigerant fluids, such as potassium formate, the temperature profile develops at a slower rate than the velocity profile Consequently the development of the temperature profile exhibits a greater influence upon the heat transfer to these fluids under developing flow conditions than does the hydrodynamic development. In Sections 4.1–4.3, the development of the fluid temperature profile upstream of, within and downstream of a 15 mm radius U-bend is examined For the model examined, the inlet temperature was specified as 250 K and an inlet mass flow rate specified as 0.06 kg/s provided $Re \approx 1000$ for the pipe diameter, $D = 10$ mm. The average fluid temperature at the pipe exit was found to be approximately 256 K. The development of secondary flows within the U-bend is discussed in addition to the impact upon the heat transfer situation. All predictions are determined using the FLUENT package. Section 4.4 discusses the influence of the bend radius upon the temperature profile development and downstream heat transfer enhancement effect. The effect of *Re*, in particular upon natural convection effects, is discussed in Section 4.5.

4.1. Upstream of the bend

Fig. 6 illustrates temperature distribution upstream of the U-bend in which developing flows in a straight tube is simulated. The flow does not achieve thermally or hydraulically fully developed conditions in the inlet pipe, however the pipe is sufficiently long to reveal the significant decrease in Nusselt number that occurs as the flow develops. Contours are shown at the inlet pipe entrance and at 10, 20 and 40 pipe diameters downstream, where the total straight pipe length is 50 pipe diameters. The fluid temperature is observed to increase steadily along the length of the pipe according to a uniform heat flux entry condition, such that fluid at the pipe walls achieves the highest temperatures while a core of colder fluid remains at the centre of the pipe. Due to the laminar nature of the flow, transverse mixing is not significant although the cold fluid at the core tends to descend towards the bottom of the pipe, while the fluid with the highest temperature is found towards the top of the pipe as a result of natural convection effects.

As the temperature at the inside surface of the pipe increases along its length, the difference between the average fluid temperature and the inside surface temperature increases. This results in a steady decrease in *Nu* number along the inlet pipe in the direction of flow. This is illustrated in Fig. 7, in which the *Nu* number preceding the bend as predicted by the FLUENT simulation, is illustrated alongside the *Nu* number as predicted by a correlation developed by Churchill and Ozoe [18], Eq. (10).

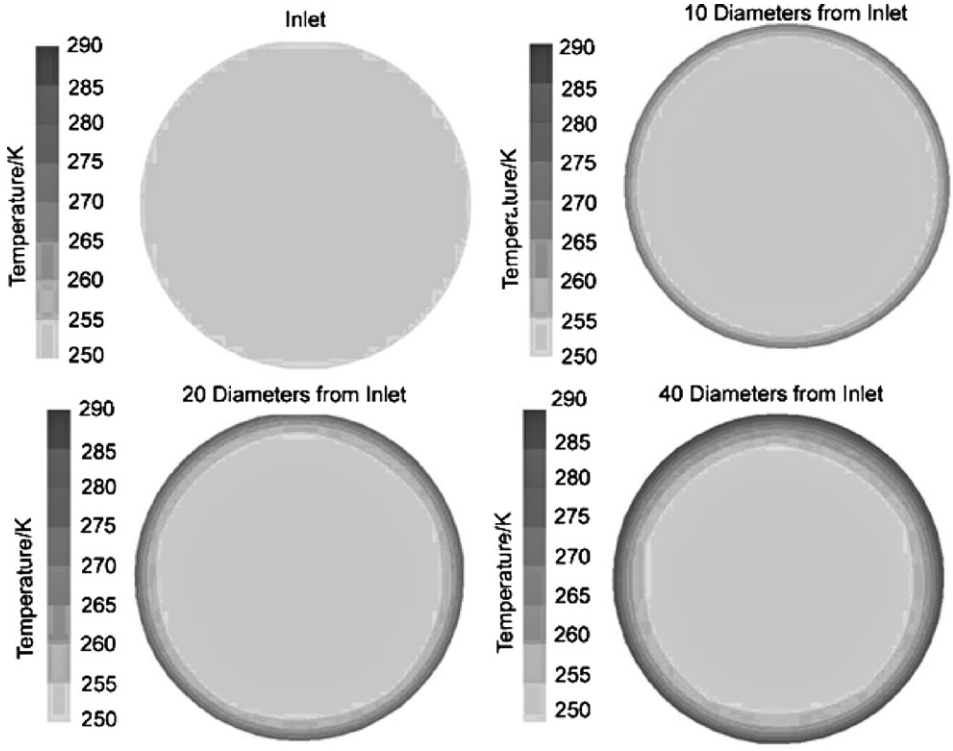

Fig. 6. Temperature contours upstream of the bend.

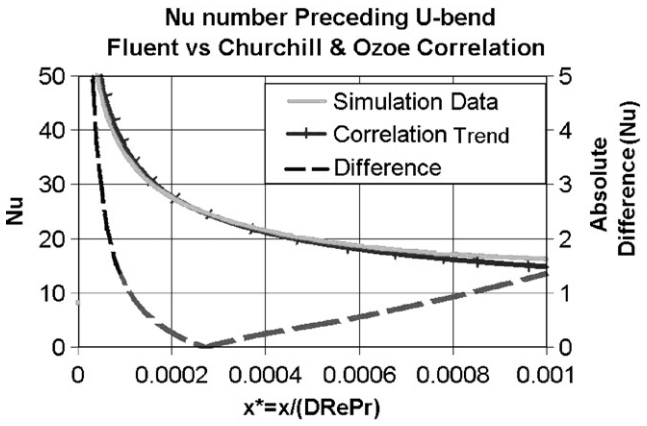

Fig. 7. *Nu* number preceding the U-bend.

$$\frac{Nu+1}{5.364[1+(Gz/55)^{10/9}]^{3/10}} = \left[1+\left(\frac{Gz/28.8}{[1+(Pr/0.0207)^{2/3}]^{1/2}[1+(Gz/55)^{10/9}]^{3/5}}\right)^{n/2}\right]^{1/n} \qquad n=2.5 \tag{10}$$

The correlation is applicable for laminar forced convection following a combined entry subject to a constant surface heat flux. For both the simulation and correlation data, the *Nu* number is observed to decrease steadily along the length of the pipe as the flow develops. The simulation results compare favourably to the correlation values. The Churchill and Ozoe correlation however, does not incorporate the effects of natural convection and as a result an increasing divergence between the two sets of data develops downstream of the pipe inlet as natural convection effects become more significant The average difference between the data sets is within 4.5% of the correlation values.

4.2. Within the bend

Fluid enters the U-bend with the temperature profile approaching a parabolic shape developed within the straight heated inlet section. Within the bend this situation rapidly changes as a result of the Dean vortices that develop within the bend. A pressure gradient develops as fluid enters the bend, before impinging on the pipe walls at the outside of the bend and final redirecting around the bend. As illustrated in Fig. 8, higher pressure is found towards the outside wall of the bend, on which the fluid impinges, while lower pressures are experienced towards the inside wall of the bend. Centrifugal forces, induced due to the rotational motion of the fluid about the bend axis, tend to drive the fast moving fluid located at the core of the flow towards the outside of the bend. Towards the pipe walls however, the fluid velocity, and thus the centrifugal forces, are significantly lower than at the centre of the pipe. As a result, towards the walls the transverse pressure gradient illustrated in Fig. 8 is sufficient to overcome the centrifugal force and to drive fluid from the bend outside around the pipe wall towards the bend inside. In Fig. 8, transverse velocity components that reveal the Dean vortices at 90° through the U-bend as predicted by the FLUENT model are also illustrated. The centres of the Dean vortices are found to be located away from the vertical axis of the pipe, towards the inside of the bend. The secondary flow however is observed to be very weak over a small region located directly at the inside wall of the bend.

Hong and Hrnjak [6] suggested that secondary flows could cause mixing, resulting in a new development length downstream of the U-bend similar to that of a combined entry. Zitny et al. [15] alternatively suggested that the heat transfer enhancement mechanism was similar to that of a flow inverter. These investigations however did not examine the impact of secondary flows upon temperature profile development directly. The effect of the secondary flow upon the temperature profile development, as predicted by the current model is illustrated in Fig. 9. Temperature contours are illustrated at three locations through the bend, 30°, 90° and 150°. The secondary flows are observed to drive cold fluid from the core of the pipe towards the outside pipe walls, with further circulation along the outside walls from the outside of the bend to the inside of the bend. This cold fluid replaces warm fluid that had developed at the pipe walls as the fluid moved through

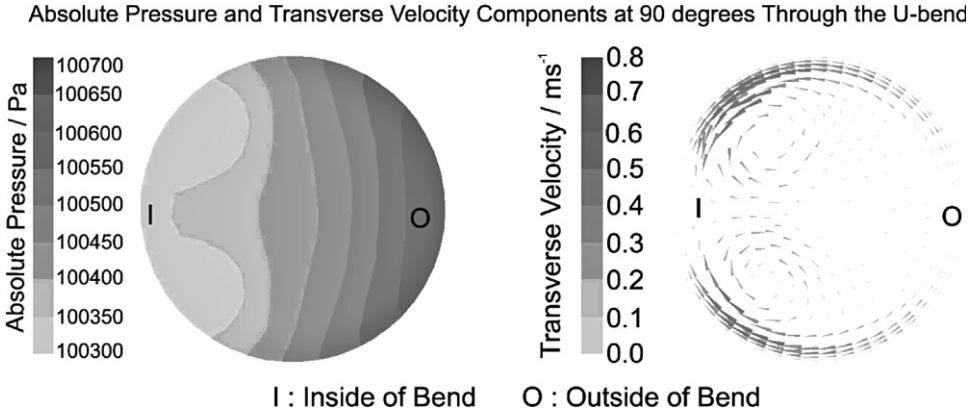

Fig. 8. Absolute pressure and transverse velocity components at 90° through the U-bend.

the inlet pipe. The warm fluid is simultaneously driven by the secondary flow, around the pipe walls towards the bend inside wall and onwards towards the pipe core. Consequently the thermal boundary layer is eliminated and a sudden drop in fluid temperature at the surface of the pipe occurs within the bend. It is this temperature drop and elimination of the thermal boundary layer that causes the subsequent heat transfer enhancement downstream of the U-bend. Notably however, the inversion process is not complete. A region of fluid with elevated temperature remains at the pipe wall located in a region towards the bend inside, *I*. The relative size of this region gives a measure of the completeness of the fluid inversion process. A more complete inversion would minimise the size of this region, potentially reducing the average fluid surface temperature and, as a result, maximising the downstream heat transfer enhancement effect. This effect is discussed in more detail in Section 4.4.

4.3. Downstream of the bend

Fig. 10 shows the transverse components of velocity at 90° through the U-bend and at one diameter downstream of the bend exit. Vectors have been scaled up by a factor of 2 for the in-bend vectors but were scaled up by a factor of 5 for the downstream vectors to ensure that they were large enough to view clearly. Upon exiting the bend, the centrifugal forces and pressure gradient that caused the secondary flow to develop within the bend are observed to have disappeared. As a result the transverse velocity components diminish swiftly downstream of the bend. For the current model, at 90° through the bend, the maximum transverse velocity was approximately 0.4 m/s. At one diameter downstream of the bend however, the maximum transverse velocity reduced to <0.1 m/s. By five diameters downstream of the bend the maximum transverse velocity reduced to approximately 0.04 m/s, 10% of the value achieved within the bend. Consequently the secondary flow had a minimal impact upon the temperature profile development beyond the bend exit.

Fig. 11 illustrates the temperature contours at the bend exit and at 10, 20 and 40 diameters downstream of the U-bend. The effect of the secondary flow was observed to diminish significantly. The fluid from the core is no longer driven from the centre of the pipe towards the pipe walls. The temperature profile instead develops in a manner consistent with that of laminar pipe flow not preceded by a bend, i.e., as the fluid progresses through the outlet pipe, the fluid close to the walls swiftly increases in temperature while fluid at a greater depth heats at a much lesser rate. Mixing by the secondary flow decreases substantially and the fluid starts to approach a parabolic temperature profile once again. Some warm fluid at the core of the pipe remains in place and can be observed in Fig. 11 to remain

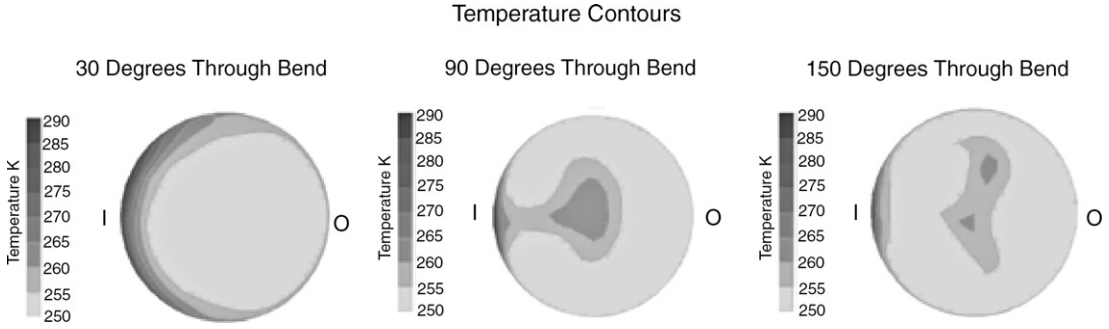

Fig. 9. Temperature contours at 30°, 90° and 150° through the U-bend.

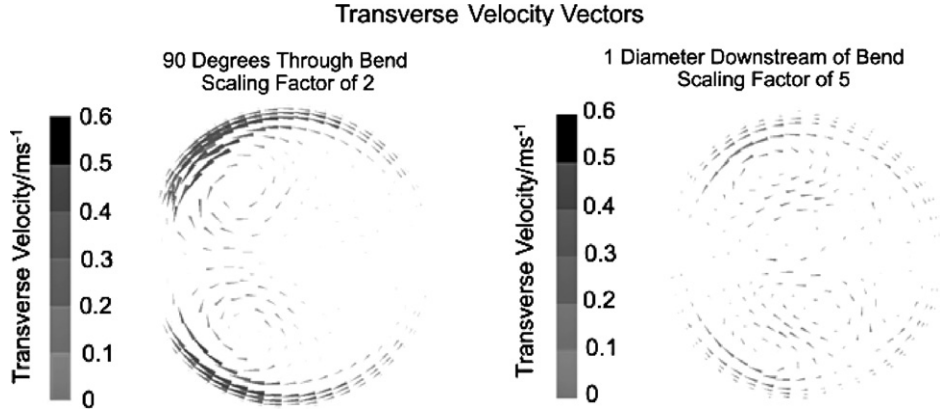

Fig. 10. Transverse velocity vectors at 90° Through the bend and at 1 diameter downstream of the bend.

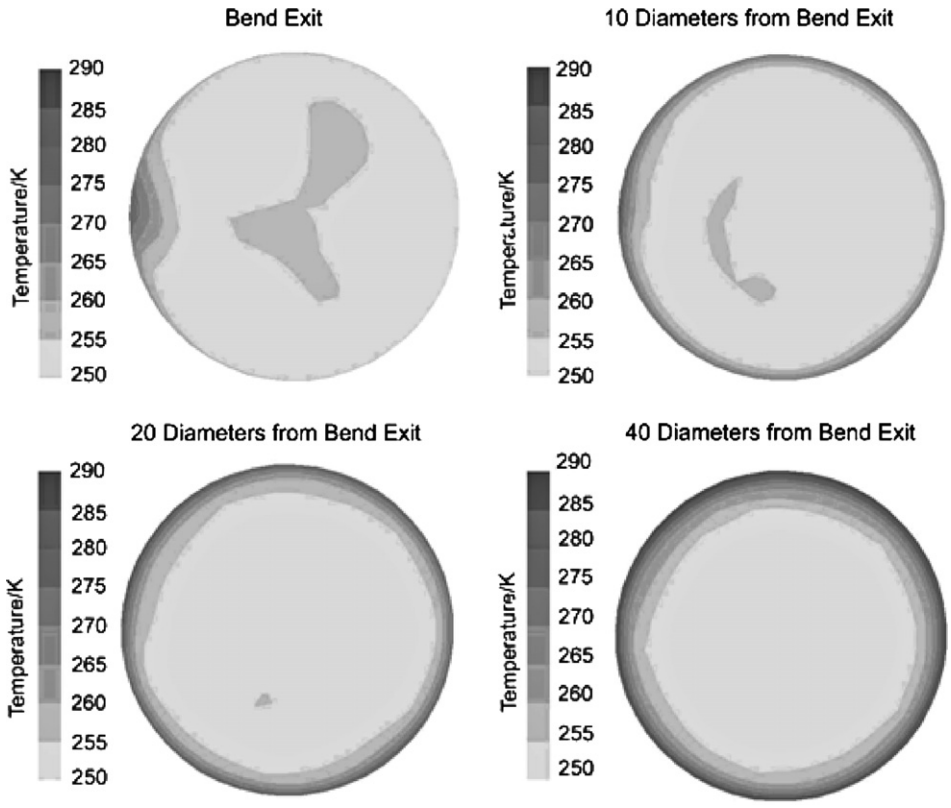

Fig. 11. Temperature contours at the bend exit and at 10D, 20D and 40D downstream.

for up to 20 diameters downstream. This warm fluid is observed to distort the developing parabolic profile somewhat, before eventually dissipating.

Hong and Hrnjak [6] suggested that the heat transfer situation downstream of a U-bend was equivalent to that of a combined entry situation. Further to this, in the investigations of Haglund Stignor [5], it was assumed that the region following a U-bend could be treated as a combined entry. However, from the current investigations, it was observed that the temperature contours at the bend exit differ significantly from the uniform temperature profile associated with a combined entry situation. As a result, it is apparent that the assumption that the heat transfer situation downstream of a U-bend is identical to that of a combined entry may not be entirely accurate.

Fig. 12 illustrates the *Nu* number values predicted by the model for the region downstream of the U-bend. These values are compared to the simulation values determined for the combined entry region upstream of the U-bend. It was found that the *Nu* number values downstream of the U-bend are not identical to those for a combined entry. The downstream *Nu* values are observed to exceed the equivalent combined entry values, remaining greater than 20% higher than the combined entry value for up to $x^* = 0.0004$ (corresponding in this case to approximately 20 diameters downstream). This phenomenon is a consequence of the temperature profile inversion process. As the fluid progresses down the pipe, both for the combined

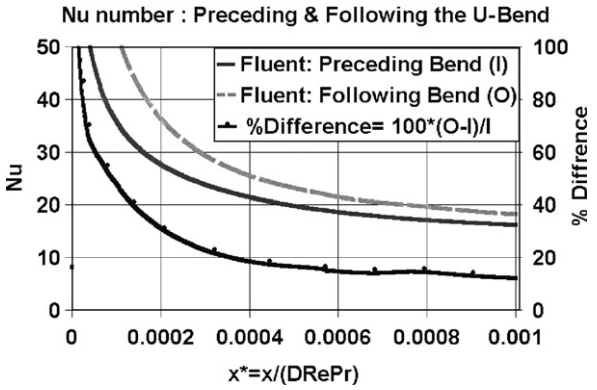

Fig. 12. *Nu* number values preceding and following the bend.

entry situation and for the region following the bend, the surface temperature increases. As a result, the difference between surface temperature and average fluid temperature increases and the convective heat transfer coefficient decreases. For the combined entry situation, cold fluid located at the core of the flow results in the swift development of an increasing difference between surface temperature and average fluid temperature as the fluid progresses down the pipe. Following the bend however, the situation is altered insofar as cold fluid re-locates to the pipe surface, while warm fluid re-locates towards the core of the pipe. This warm fluid ensures that the difference between average

fluid temperature and surface temperature increases at a lesser rate for the region following a bend than it does for a combined entry situation. Consequently, the surface heat transfer coefficient and *Nu* number values downstream of a U-bend exceed those achieved for a combined entry situation.

4.4. Influence of varying bend radius

From the definition of the Dean number, $K = Re\sqrt{(r/R)}$, it can be concluded that the ratio of the pipe to bend radius, (r/R) influences the secondary flow developed within the bend and therefore may also influence the downstream heat transfer enhancement. A number of models were developed using FLUENT with various values of bend radius ($R = 12.5$, 15 and 20 mm) and a constant Re ($Re \approx 1000$) in order to investigate this effect. Fig. 13 illustrates the ratio of *Nu* predicted by the simulation to *Nu* number for a combined entry as predicted by the Churchill and Ozoe correlation. This reveals the variation in the enhancement effect downstream of the bend as bend radius varies from 20 to 12.5 mm. The maximum average *Nu* enhancement over correlation values for a combined entry was observed to be 31% and was achieved for $R = 20$ mm (corresponding to a value for $r/R = 0.25$). For $R = 15$ mm and $R = 12.5$ mm, the average percentage enhancement over combined entry values were 28% and 26%, respectively. The upward turn in the trends beyond $x^* \approx 0.0006$ reveals the impact of natural convection, which is not taken into account by the correlation. If natural convection effects were incorporated into the correlation, or conversely if no natural convection effects were present, the downstream enhancement effect could be expected to continue to descend towards a steady zero percent asymptote as the flow approaches fully developed conditions.

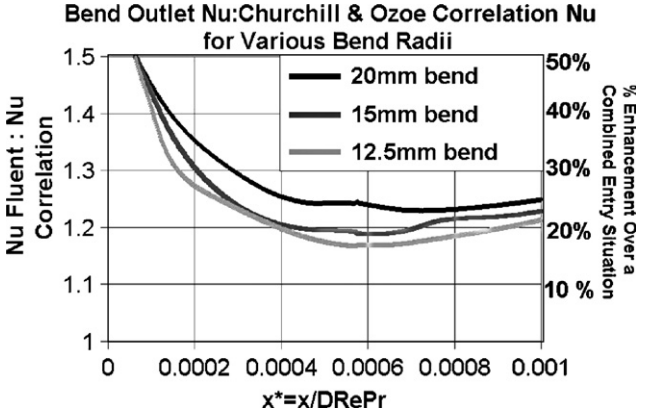

Fig. 13. Ratio of simulation *Nu* number following the bend at various bend radii to Nu number for a combined entry, predicted by the Churchill and Ozoe correlation.

The trend of these results does not agree with the trends suggested by the correlation for heat transfer following a U-bend developed by Abdelmessih and Bell [10]. The correlation suggested that increasing K leads to an increase in downstream heat transfer. The results of this investigation into the effects of bend radius, have suggested that decreasing K as a result of increased bend radius can, for laminar flow of secondary refrigerants around bends with radii typical of air chillers, result in increased downstream heat transfer enhancement.

An explanation for this variation in the magnitude of the heat transfer enhancement may be obtained by examining the temperature at the exit of each of the various bends, as illustrated in Fig. 14. The temperature profiles are somewhat similar to each other, cold fluid has been driven towards the pipe surface by the secondary flow while some warm fluid has been driven towards the centre of the pipe. A region of particular interest however is the region of elevated temperature located towards the inside of the bend. The angle θ is a measure of the size of this region and is the angle of the sector of the cross-section for which the surface temperature of the pipe exceeds 265 K. The reference temperature was selected as 265 K because it was the mean of the maximum and minimum surface temperatures experienced at the bend exit for these simulations (temperature ranges from 250 to 280 K). A large value for θ indicates that a greater part of the surface experiences an elevated temperature. This tends to increase average surface temperature, thus decreasing the heat transfer enhancement effect. In Fig. 14 it can be observed that the value for θ increases from $\theta \approx 30°$ for $R = 20$ mm to $\theta \approx 45°$ for $R = 12.5$ mm. Further to the impact upon the region of elevated temperature, it is observed in Fig. 14 that the bend radius has an impact upon the shape of the warm

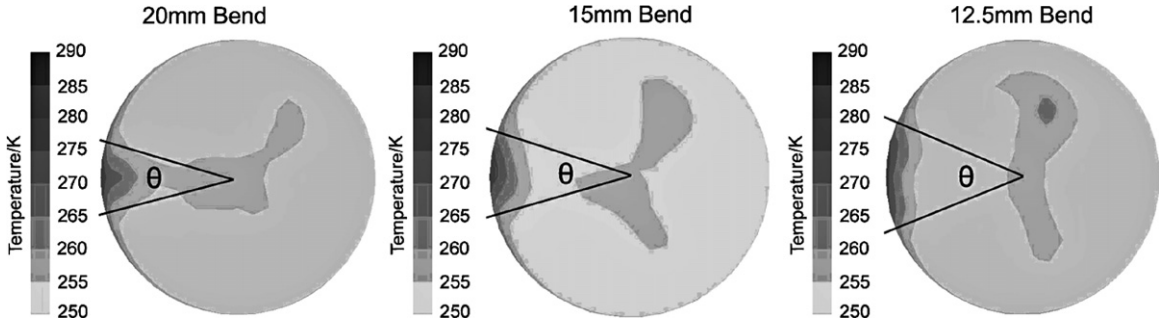

Fig. 14. Temperature contours at the bend exit for various bend radii.

fluid core at the bend exit. For smaller bend radii, the warm core is more elongated in the vertical plane. This may be an effect of a stronger secondary flow experienced for the tighter bend, which may be sufficiently strong to drive warm fluid beyond the centre of the pipe and back towards the pipe walls. An ideal temperature profile inversion would drive warm fluid as close to the centre of the pipe as possible. Thus the more elongated warm core, which places more warm fluid closer to the pipe walls, is not desirable. While the shape of the warm fluid core could potentially have an impact on the enhancement effect, it is the difference in the region of elevated temperature for the models investigated that is suggested here to be the primary underlying phenomenon that accounts for the variation in downstream heat transfer enhancement evident in Fig. 13.

4.5. Influence of varying Reynolds number

Forced convective heat transfer is typically improved by using higher *Re* numbers, this however comes at the expense of an increased pressure drop penalty along the pipes and an associated increase in pumping energy requirements. Haglund Stignor[5] suggested that, due to the reduced pumping energy requirements, laminar flow of secondary refrigerants can be the most energy efficient option for heat exchanger geometry designs that take into account the positive impact of U-bends. The investigation outlined in Sections 4.1–4.4 have thus examined secondary refrigerant fluid flow for a laminar flow operating condition, $Re = 1000$. Similar models were also developed for $Re = 500$ and $Re = 1500$. These models are not discussed in detail here, however it should be noted that their results are consistent with those already discussed regarding the mechanism that causes heat transfer enhancement downstream of U-bends, the inversion of temperature profiles and the impact of varying bend radius.

Fig. 15 illustrates the *Nu* number following a 15 mm U-bend for the three *Re* number values investigated, plotted against the dimensionless distance x^*. For all x^*, the greatest value for *Nu* number was achieved for $Re = 500$ while little difference is observed between the trends for $Re = 1000$ and $Re = 1500$. For heated, low *Re* number flows, a combination of low axial velocities and significant transverse temperature gradients can lead to increased mixing by natural convection ultimately resulting in improved heat transfer. The impact of natural convection at various different *Re* number values is further illustrated in Fig. 16 in which the value for Gr/Re^2 is illustrated for $Re = 500$, $Re = 1000$ and $Re = 1500$. It is shown that at $Re = 500$, for all x^*, Gr/Re^2 is approximately four times the equivalent value for $Re = 1000$, which itself is approximately double the value achieved for $Re = 1500$. This result reveals the impact of natural convection effects, which can in particular influence the heat transfer situation at the lower *Re* numbers investigated.

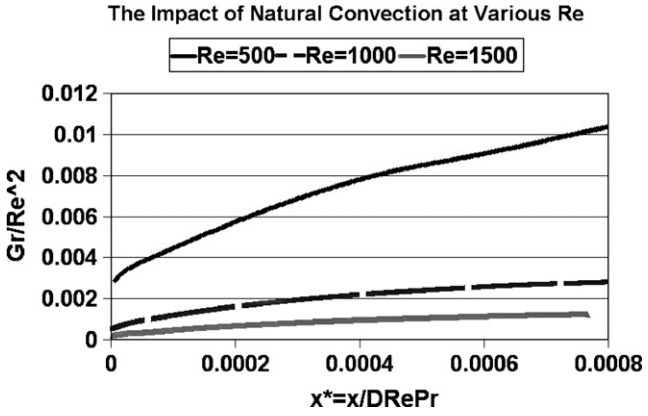

Fig. 16. Impact of natural convection at $Re = 500$, $Re = 1000$ and $Re = 1500$.

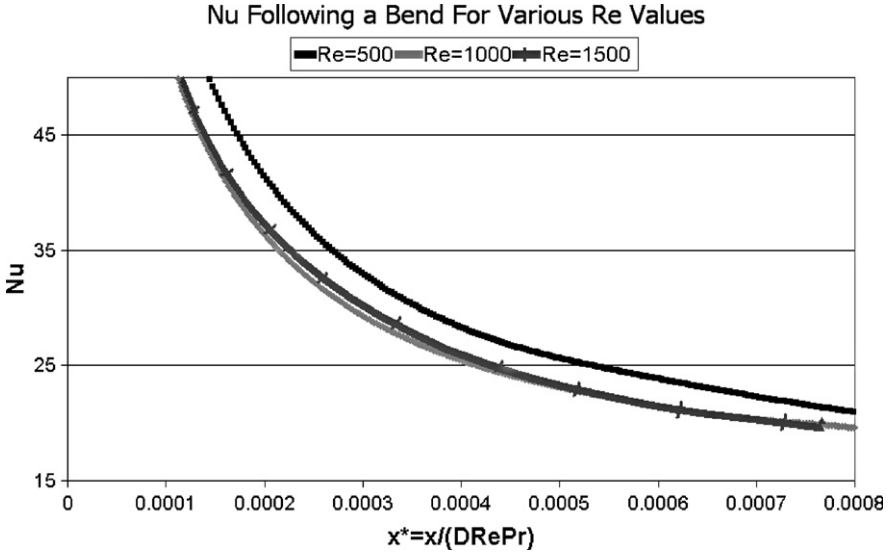

Fig. 15. *Nu* number following a 15 nm U-bend for $Re = 500$, $Re = 1000$ and $Re = 1500$.

5. Conclusions

This work was motivated by the requirement for a greater understanding of the mechanism by which U-bends enhance downstream heat transfer from laminar flow secondary refrigerants in air-chillers. This work is of particular interest with regard to heat transfer from secondary refrigerants in finned tube air-chillers and other applications where high *Pr* number, single phase fluids are used for heat transfer applications in tubes that incorporate return U-bends. A model of a heat exchanger U-bend was developed using the FLUENT CFD software package to investigate the development of temperature profiles upstream of, within and downstream of a U-bend for a laminar flow secondary refrigerant. Validation of the model heat transfer was carried out by comparison with data from the literature. The mechanisms by which U-bends enhance refrigerant side heat transfer downstream of a secondary refrigerant air-chiller U-bend were examined. It was shown that centrifugally induced secondary flows, known as Dean vortices, partially invert the temperature profile. Cold fluid is driven from the core of the pipe towards the pipe walls while warm fluid is driven around the circumference of the pipe towards the inside of the bend and onwards towards the centre of the pipe. Consequently, at the bend exit, cold fluid existed at the pipe walls and warm fluid was located at the core of the flow. Thus, the surface temperature of the pipe dropped significantly within the bend, resulting in an improved heat transfer situation downstream. It had been suggested previously Hong and Hrnjak [6] that heat transfer following a U-bend was very similar to that associated with a combined entry. In this work however, in some circumstances, *Nu* values downstream of a U-bend were found to exceed *Nu* values for a combined entry situation by greater than 20% for up to 20 pipe diameters downstream. A region of elevated temperature, which increased average surface temperature and thus decreased the downstream heat transfer enhancement effect, was observed towards the inside of the bend. θ, the angle of the sector of the bend exit cross-section for which in this case the surface temperature remained above 265 K, was used to characterise the region of elevated temperature. It was found that minimising the value of θ, for example by optimising the size of the bend radius, resulted in the greatest enhancement effect downstream of the bend. The effect of varying bend radius was investigated for models with bend radii of 12.5, 15, and 20 mm. The smallest value of θ was achieved for $R = 20$ mm, for which $\theta \approx 30°$ at $Re = 1000$, while for $R = 12.5$ mm, $\theta \approx 45°$. The increase in θ was accompanied by an associated decrease in downstream heat transfer enhancement. For some low *Re* number flows investigated natural convection effects were found to further enhance heat transfer downstream of a U-bend. For all dimensionless distance examined, the greatest *Nu* number values were achieved for the lowest *Re* number value investigated, $Re = 500$.

Acknowledgement

This paper was prepared with the support of the University College Dublin School of Electrical, Electronic and Mechanical Engineering Demonstratorship scholarship fund.

References

[1] W.T. Horton, E.A. Groll, Secondary Loop Refrigeration in Supermarket Applications: A Case Study, International Congress of Refrigeration, ICR0434 Washington, DC, 2003.
[2] S. Sawalha, B. Palm, Energy Consumption Evaluation of Indirect Systems with CO_2 as a Secondary Refrigerant in Supermarket Refrigeration, International Congress of Refrigeration, ICR0434 Washington, DC, 2003.
[3] H. Kruse, Refrigerant use in Europe, ASHRAE J. 42 (9) (2004) 16–24.
[4] W.J. Terrell Jr., Y. Mao, P.S. Hrnjak, Evaluation of Secondary Fluids for Use in Low-temperature Supermarket Application, ACRC CR-15, University of Illinois, Urbana, IL, 1999.
[5] C. Haglund Stignor, Liquid side heat transfer and pressure drop in Finnned-tube cooling coils, Thesis for the Degree of Licentiate of Engineering, Lund Institute of Technology, 2002.
[6] S.H. Hong, P. Hrnjak, Heat transfer in thermally developing flow of fluids with high Prandtl numbers preceding and following U-bend, ACRC Report CR-24, University of Illinois, Urbana, IL, 1999.
[7] A.J. Ede, The effect of a 180° bend on heat transfer to water in a tube, in: Proceedings of the Third International Heat Transfer Conference, Chicago, 1966, pp. 99–104 .
[8] M. Moshfeghian, Fluid flow and heat transfer in U-bends, PhD Thesis, Oklahoma State University, Stillwater, 1978.
[9] N.D. Mehta, Laminar flow heat transfer in a tube preceded by a 180° bend, MSc Thesis, Oklahoma State University, Stillwater, 1979.
[10] A. Abdelmessih, K. Bell, Effect of mixed convection and U-bends on the design of double-pipe heat exchangers, Heat Transfer Eng. 20 (3) (1999) 25–36.
[11] W.R. Dean, Note on the motion of fluid in a curved pipe, Philos. Magazine 4 (20) (1927) 208–223.
[12] W.R. Dean, The stream line motion of fluid in a curved pipe, Philos. Magazine 5 (30) (1928) 673–695.
[13] H. Ito, Flow in curved pipes, JSME Int. J. 30 (262) (1987) 543–552.
[14] E.N. Sieder, G.E. Tate, Heat transfer and pressure drop of liquids in tubes, Indus. Eng. Chem. 28 (12) (1936) 1429–1435.
[15] R. Zitny, T.C.T. Luong, P. Strasak, J. Sestak, Heat transfer enhancement and RTD in pipes with flow inversion, Heat Transfer Eng. 25 (4) (2004) 67–79.
[16] T. Blacker, M.B. Stephenson, Paving: a new approach to automated quadrilateral mesh generation, Int. J. Num. Meth. Eng. 32 (1991) 811–847.
[17] T. Blacker, The cooper tool, in: Proceedings of the Fifth International Meshing Roundtable, 1996, pp. 13–30.
[18] S.W. Churchill, H. Ozoe, Correlations for laminar forced convection with uniform heating in flow over a plate and in developing and fully developed flow in a tube, Trans. ASME J. Heat Transfer 95 (1973) 78–84.